

A Novel Wideband Spectrum Sensing System for Distributed Cognitive Radio Networks

Hongjian Sun[†], Arumugam Nallanathan[†], Jing Jiang[‡], David I. Laurenson[‡],
Cheng-Xiang Wang[¶], and H. Vincent Poor[§]

[†]Department of Electronic Engineering, King's College London, London, WC2R 2LS, UK

[‡]Institute for Digital Communications, University of Edinburgh, Edinburgh, EH9 3JL, UK

[¶]School of Engineering & Physical Sciences, Heriot-Watt University, Edinburgh, EH14 4AS, UK

[§]Department of Electrical Engineering, Princeton University, Princeton, NJ 08544, USA

Email: hongjian.sun@kcl.ac.uk; nallanathan@ieee.org; {j.jiang, dave.laurenson}@ed.ac.uk;

Cheng-Xiang.Wang@hw.ac.uk; poor@princeton.edu

Abstract—A significant challenge of cognitive radio (CR) is to perform wideband spectrum sensing in a fading environment. In this paper, a novel multi-rate sub-Nyquist spectrum detection (MSSD) system is introduced for cooperative wideband spectrum sensing in a distributed CR network. Using only a few sub-Nyquist samples, MSSD is able to sense the wideband spectrum without full spectrum recovery. Specifically, given the low spectral occupancy, sub-Nyquist sampling is performed in each sampling channel and a test statistic is formed by using sub-Nyquist samples from multiple sampling channels. Furthermore, the use of different sub-Nyquist sampling rates is proposed to improve the system detection performance, and the performance of MSSD over both non-fading and Rayleigh fading channels is analyzed. Numerical results show that MSSD can considerably improve the wideband spectrum sensing performance in a fading scenario, with a relatively low implementation complexity and a low computational complexity.

I. INTRODUCTION

Radio frequency (RF) spectrum is a precious and scarce natural resource for wireless communication systems. However, the report published by Federal Communication Commission (FCC) has shown that most licensed spectrum is under-utilized [1]. Recently, cognitive radio (CR) [2] has emerged as one of the most promising candidates for improving the spectral utilization efficiency [3]–[6]. Spectrum sensing is one of the most critical components in a CR system, enabling the CR to access the licensed spectrum when it is not used by primary users (PUs). In order to exploit more spectrum opportunities, CR requires a wideband spectrum sensing structure. Meanwhile, due to the effects of multipath/shadow fading, cooperative spectrum sensing has been considered for increasing the reliability of spectrum sensing [7]–[9]. In practice, cooperative wideband spectrum sensing in a distributed CR network is difficult

H. Sun, and A. Nallanathan acknowledge the support of the UK Engineering and Physical Sciences Research Council (EPSRC) with Grant No. EP/I000054/1. J. Jiang, D. I. Laurenson, and C.-X. Wang acknowledge the support from the Scottish Funding Council for the Joint Research Institute in Signal and Image Processing between the University of Edinburgh and Heriot-Watt University, as part of the Edinburgh Research Partnership in Engineering and Mathematics (ERPEm). C.-X. Wang also acknowledges the support of the RCUK for the UK-China Science Bridges Project: R&D on (B)4G Wireless Mobile Communications.

to realize, due to both high implementation/computational complexity and high financial/energy costs.

Previous work has focused on the implementation of wideband spectrum sensing. Tian and Giannakis [10] proposed a wavelet detection approach. It provides an advantage of flexibility in adapting to a dynamic wideband spectrum. However, characterizing the wideband spectrum requires an analog-to-digital converter (ADC) with a high sampling rate, and the energy cost for both the ADC and the digital signal processor (DSP) is prohibitive. In [11], and [12], Quan *et al.* presented a multiband joint detection (MJD) approach for jointly detecting the wideband spectrum over multiple frequency bands. It was shown that MJD performs well under practical conditions. In [13], a filter-bank system for wideband spectrum sensing was presented, but it was noted that the implementation of a filter-bank system requires a large number of radio frequency components [14]. As the spectrum occupancy is low, compressed sensing (CS)-based techniques were introduced to implement wideband spectrum sensing by sub-Nyquist sampling [14]–[16]. An implementation issue of this approach is that a separate compression device is required in each sampling channel, and the synchronization of these devices must be addressed. Another problem is that the full spectrum reconstruction requires a high computational complexity, which results in a high spectrum sensing overhead.

This paper presents a multi-rate sub-Nyquist spectrum detection (MSSD) system for wideband spectrum sensing in a distributed CR network. The proposed system can sense the wideband spectrum by using only a few sub-Nyquist samples without reconstructing the full spectrum, which leads to a low implementation/computational complexity. Specifically, in MSSD, sub-Nyquist sampling is performed in each sampling channel to wrap the sparse spectrum onto itself. Spectral energy is calculated by using sub-Nyquist samples in each sampling channel. A final test statistic is formed by using energy vectors from all distributed CRs. We then propose to use different sampling rates to optimize the detection performance. In addition, we analyze the performance of MSSD over both non-fading and Rayleigh fading channels, and derive

closed-form bounds for the probabilities of false alarm and detection. Compared with existing spectrum sensing methods, MSSD improves wideband spectrum sensing performance, with a lower implementation complexity and a lower spectrum sensing overhead.

This paper is organized as follows. In Section II, we introduce the signal model for spectrum sensing. In Section III, we present a novel MSSD system for cooperative wideband spectrum sensing. Numerical results are presented in Section IV, with conclusions given in Section V.

II. SIGNAL MODEL

In this paper, we model the spectrum sensing on a frequency bin n ($n = 1, 2, \dots, N - 1$) as a hypothesis test choosing between $\mathcal{H}_{0,n}$ (absence of a PU) and $\mathcal{H}_{1,n}$ (presence of a PU). That is, we test the following binary hypotheses:

$$X[n] = \begin{cases} Z[n], & \mathcal{H}_{0,n} \\ H_n S[n] + Z[n], & \mathcal{H}_{1,n} \end{cases} \quad (1)$$

where $\vec{X} \in \mathbb{C}^N$ is the discrete Fourier transform of Nyquist samples, H_n stands for the discrete frequency response between the PU and the CR, $S[n]$ is the primary signal transmitted on frequency bin n , and $Z[n]$ is complex additive white Gaussian noise (AWGN) with zero mean. For simplicity, in the rest of the paper we assume that the noise variance of the spectrum is normalized to be 1, i.e., $Z[n] \sim \mathcal{CN}(0, 1)$.

As an energy detector does not require prior information and has low complexity [17], we calculate the signal energy over an interval of J samples by

$$E_s[n] = \sum_{j=0}^{J-1} |X_j[n]|^2, \quad n = 0, 1, \dots, N - 1 \quad (2)$$

where $X_j[n]$ denotes j -th spectral observation. The decision rule of the energy detector is given by

$$\begin{array}{ll} \mathcal{H}_{1,n} \\ E_s[n] \gtrless \lambda_n, \quad n = 0, 1, \dots, N - 1 \\ \mathcal{H}_{0,n} \end{array} \quad (3)$$

where λ_n is a detection threshold for the frequency bin n .

Following [18], the signal energy can be modeled by

$$E_s[n] \sim \begin{cases} \chi_{2J}^2, & \mathcal{H}_{0,n} \\ \chi_{2J}^2(2\gamma[n]), & \mathcal{H}_{1,n} \end{cases} \quad (4)$$

where $\gamma[n]$ denotes the signal-to-noise ratio (SNR) at the CR on the frequency bin n , and χ_{2J}^2 and $\chi_{2J}^2(2\gamma[n])$ denote central and non-central chi-square distributions, respectively. Both distributions have $2J$ degrees of freedom, and the latter one has a non-central parameter $2\gamma[n]$. The probabilities of false alarm and detection can be obtained as [18]

$$P_{f,n} = \Pr(E_s[n] > \lambda_n | \mathcal{H}_{0,n}) = \frac{\Gamma(J, \frac{\lambda_n}{2})}{\Gamma(J)} \quad (5)$$

and

$$P_{d,n} = \Pr(E_s[n] > \lambda_n | \mathcal{H}_{1,n}) = Q_J(\sqrt{2\gamma[n]}, \sqrt{\lambda_n}) \quad (6)$$

respectively, where $\Gamma(a)$ is the gamma function, $\Gamma(a, x)$ is the upper incomplete gamma function, and $Q_J(a, x)$ denotes the generalized Marcum Q-function.

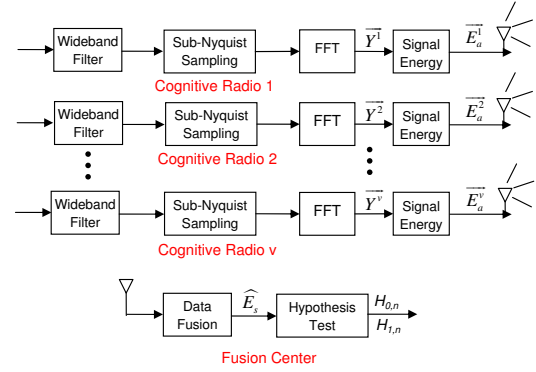


Fig. 1. Block diagram of multi-rate sub-Nyquist spectrum detection in a distributed CR network.

III. PROPOSED SPECTRUM SENSING SCHEME

We assume that v spatially distributed CRs collaborate for wideband spectrum sensing. All CRs keep quiet during the spectrum sensing interval as imposed, e.g., by a medium access control (MAC) layer protocol. In a short observation time, the spectra viewed by CRs are assumed to be quasi-stationary. The full spectrum vector, i.e., \vec{X}_j , is k -sparse ($k \ll N$), which means only the largest k out of N components are non-neglectable (due to low spectral occupancy [19]). In a carrier sense, this means that there are only a few active carriers even though most of them are allocated to different wireless systems. The sparsity level, i.e., k , can be obtained from initialization, e.g., coarse spectrum scanning [20], and will not be addressed here. In addition, we assume that the spectral support (a set of frequency bins that are occupied by PUs) in different CRs is correlated due to similar radio environments. In this paper, we are interested in identifying a w -out-of- v ($w \in [1, v]$) spectral support (i.e., in w or more than w CRs, the same frequency bin is occupied by PUs).

A. System Model

In MSSD, as shown in Fig. 1, each CR is equipped with one wideband filter, one low-rate sampler, and a fast Fourier transform (FFT) device for calculating signal energy in the frequency domain. The wideband filters prior to the samplers remove frequencies outside the spectrum of interest, and are altered to have the same bandwidth, W . The work procedure of MSSD can be described as:

- 1) The fusion center (FC) distributes different sub-Nyquist sampling rates to CRs. In an observation time T , the number of samples in CRs, i.e., M^1, \dots, M^v , are set to be v consecutive primes, where $M^i \sim \mathcal{O}(\sqrt{N})$.
- 2) CRs perform asynchronous sub-Nyquist samplings (subject to that the observed spectra within time offset are quasi-stationary).
- 3) An FFT is used to calculate the spectrum \vec{Y}^i ($i \in [1, v]$).
- 4) The signal energy, i.e., E_a^i , is calculated over an interval of J samples in all CRs, by using \vec{Y}^i .
- 5) Each CR quantizes the signal energy and transmits it to FC.

- 6) The FC fuses received data to form a test statistic, i.e., \widehat{E}_s .
- 7) The FC chooses a detection threshold, λ_n , and tests binary hypotheses for all frequency bins.
- 8) The FC sends the detection results to all distributed CRs.

B. Multi-channel Sub-Nyquist Sampling

In this section, we will analyze the performance of multi-channel sub-Nyquist sampling. It is well known that the relationship between the aliased spectrum (due to sub-Nyquist sampling) and the full spectrum can be represented by (equation (59) in [21])

$$Y_j^i[m] = \frac{M^i}{N} \sum_{l=-\infty}^{\infty} X_j^i[m + lM^i] \quad (7)$$

where $\overrightarrow{Y_j^i} \in \mathbb{C}^{M^i}$ and $\overrightarrow{X_j^i} \in \mathbb{C}^N$ denote the sub-Nyquist spectrum and full spectrum of the j -th observation in the CR i , respectively. M^i and N are the number of samples within T under the sub-Nyquist rate and the Nyquist rate, respectively.

Without loss of generality, we use Ω^i and Ω_a^i to denote the spectral support in $X_j^i \in \mathbb{C}^N$ and $\overrightarrow{Y_j^i} \in \mathbb{C}^{M^i}$ as

$$\Omega^i = \{n_1, n_2, \dots, n_k\} \subset \{0, 1, \dots, N-1\} \quad (8)$$

$$\Omega_a^i = \{m_1, m_2, \dots, m_k\} \subset \{0, 1, \dots, M^i-1\} \quad (9)$$

where Ω_a^i and Ω^i can be related by

$$m_j = |n_j|_{\text{mod}(M^i)}, \quad n_j \in \Omega^i, m_j \in \Omega_a^i, j \in [1, k]. \quad (10)$$

As $k \ll N$ and $M^i \sim \mathcal{O}(\sqrt{N})$, it can be easily shown that the probability of signal overlap in $Y_j^i[m]$ is very small. When only a single signal appears on the frequency bin m , the following equation approximately holds from (7):

$$Y_j^i[m] = \frac{M^i}{N} X_j^i[m + lM^i]. \quad (11)$$

In such a scenario, with the aid of (11), the scaled aliased spectrum can be approximately modeled by

$$\sqrt{\frac{N}{M^i}} Y_j^i[m] \sim \begin{cases} \mathcal{CN}(0, 1), & m \notin \Omega_a^i \\ \mathcal{CN}\left(\sqrt{\frac{M^i}{N}} H_n^i S^i[n], 1\right), & m \in \Omega_a^i \end{cases} \quad (12)$$

where H_n^i denotes the discrete frequency response between the PU and CR i , and $S^i[n]$ is the primary transmitted signal that is received by CR i . Note that $\sqrt{\frac{N}{M^i}}$ in (12) is used to scale the sub-Nyquist spectrum vector so that it has a similar noise level to the Nyquist case.

The signal energy in CR i , i.e., $E_a^i[m] = \sum_{j=1}^J |Y_j^i[m]|^2$, can be modeled by using (12) as

$$\frac{N}{M^i} E_a^i[m] \sim \begin{cases} \chi_{2J}^2, & m \notin \Omega_a^i \\ \chi_{2J}^2 \left(2 \frac{M^i}{N} \gamma^i[n]\right), & m \in \Omega_a^i \end{cases} \quad (13)$$

where $\gamma^i[n]$ denotes SNR at CR i on the frequency bin n . The signal energy in distributed CRs will then be collected at the FC. A final test statistic, i.e., $\widehat{E}_s[n]$, is formed by

$$\widehat{E}_s[n] = \sum_{i=1}^v \frac{c^i N}{M^i} E_a^i[m + lM^i], \quad n \in [0, N), m \in [0, M^i) \quad (14)$$

where l denotes all integers within $[0, N/M^i - 1]$, and c^i is a scaling coefficient for CR i . As the noise variance in distributed CRs is often different, the scaling coefficient c^i can be used for noise-balancing when performing data fusion. We use the following decision rule:

$$\begin{aligned} \widehat{E}_s[n] &\stackrel{\mathcal{H}_{1,n}}{\gtrless} \lambda_n, \quad n = 0, 1, \dots, N-1. \\ &\stackrel{\mathcal{H}_{0,n}}{\lessgtr} \end{aligned} \quad (15)$$

Assume that Ω_M^i represents a set of mirrored frequencies (frequencies that are not occupied by PUs, but that appear to be active due to aliased components from sub-Nyquist sampling), and Ω_U^i represents a set of unaffected and unoccupied frequencies as follows:

$$\Omega_M^i \triangleq \{n | n = m + lM^i, m \in \Omega_a^i, n \notin \Omega^i\} \quad (16)$$

and

$$\Omega_U^i \triangleq \{n | n = m + lM^i, m \notin \Omega_a^i, n \notin \Omega^i\}. \quad (17)$$

Using (13), the test statistic in (14) can be modeled as

$$\widehat{E}_s[n] \sim \begin{cases} \chi_{2Jv}^2, & n \in \Omega_U \\ \chi_{2Jv}^2 \left(\frac{2}{N} \sum_{\substack{j=p \\ j=1 \\ i_j \in [1, v]}}^{j=p} c^{i_j} M^{i_j} \gamma^{i_j}[n] \right), & n \in \Omega_M \\ \chi_{2Jv}^2 \left(\frac{2}{N} \sum_{i=1}^{i=v} c^i M^i \gamma^i[n] \right), & n \in \Omega \end{cases} \quad (18)$$

where $\Omega_U \triangleq \bigcap_{i=1}^v \Omega_U^i$, $\Omega_M \triangleq \bigcup_{i=1}^v \Omega_M^i$, and $p \in [1, v]$ denotes the number of CRs that have mirrored frequencies on $n \in \Omega_M$. Note that as spectral supports in different CR nodes are different, we are interested in sensing a w -out-of- v ($w \in [1, v]$) spectral support. For simplicity, we will study the performance for $w = v$, i.e., $\Omega \triangleq \bigcap_{i=1}^v \Omega^i$. This can be easily generalized to the case of any $w \in [1, v]$ by replacing v with w in the non-centrality parameter. We note that the parameter p is dependent upon several factors, e.g., the sampling rates in the CRs, and the spectral support. For instance, if sub-Nyquist sampling rates of all CRs are the same, p will be equal to v . In such a scenario, it is difficult to distinguish between $\widehat{E}_s[n]$ ($n \in \Omega_M$) and $\widehat{E}_s[n]$ ($n \in \Omega$). However, p can be minimized by using different sampling rates in different CRs.

C. Multi-rate Sub-Nyquist Spectrum Detection

In this section, we propose to use different sampling rates in CRs to optimize the detection performance. Firstly, we consider the case of $k = 1$, which means that only one location $n_1 \in \Omega$ is occupied by the PU, then Lemma 1 will hold:

Lemma 1: If the numbers of samples in multiple CRs, M^1, M^2, \dots, M^v , are different prime numbers, and satisfy

$$M^i M^j > N, \quad \forall i \neq j \in [1, v], \quad (19)$$

then two or more CRs cannot have mirrored frequencies in the same location of $g \in \Omega_M$.

Proof: The numbers of samples in CR i and j are assumed to be M^i and M^j , respectively. According to (10) and (16),

the mirrored locations that are projected from $n_1 \in \Omega$ are given by

$$\begin{aligned} g_i &= |n_1|_{\text{mod}(M^i)} + lM^i = n_1 - hM^i + lM^i, \quad h \neq l \\ g_j &= |n_1|_{\text{mod}(M^j)} + \check{l}M^j = n_1 - \check{h}M^j + \check{l}M^j, \quad \check{h} \neq \check{l} \end{aligned} \quad (20)$$

where integers h and \check{h} are quotients from the modulo operation, and $l - h \in [-\lceil \frac{N}{M^i} \rceil + 1, \lceil \frac{N}{M^i} \rceil - 1]$, $\check{l} - \check{h} \in [-\lceil \frac{N}{M^j} \rceil + 1, \lceil \frac{N}{M^j} \rceil - 1]$.

To avoid $g_i = g_j$, which is equivalent to avoiding $(l - h)M^i = (\check{l} - \check{h})M^j$, we simply assume that M^i and M^j are different primes, and $\max(|l - h|) < M^j$, i.e. $\lceil \frac{N}{M^i} \rceil - 1 < M^j$. The condition $M^i M^j > N$ will satisfy this. Furthermore, if this holds for two CRs, the case for more than two CRs also holds. \square

Secondly, we find that when $k \geq 2$, the parameter p in (18) will be bounded by k when the conditions in Lemma 1 can be satisfied. This is because only one CR node can map the frequency $n_j \in \Omega$ to the mirrored frequency $g \in \Omega_M$, and the number of components in Ω is k .

Theorem 1: In MSSD, if the numbers of samples within T in multiple CRs, M^1, M^2, \dots, M^v , are different prime numbers, and satisfy

$$M^i M^j > N, \quad \forall i \neq j \in [1, v], \quad (21)$$

then using the decision rule of (15), the probabilities of false alarm and detection can be bounded as

$$\frac{\Gamma(Jv, \frac{\lambda_n}{2})}{\Gamma(Jv)} \leq P_{f,n} \leq Q_{Jv} \left(\sqrt{\frac{2}{N} \sum_{\substack{j=1 \\ i_j \in [1, v]}}^{j=k} c^{i_j} M^{i_j} \gamma^{i_j}[n]}, \sqrt{\lambda_n} \right) \quad (22)$$

and

$$P_{d,n} \geq Q_{Jv} \left(\sqrt{\frac{2}{N} \sum_{i=1}^v c^i M^i \gamma^i[n]}, \sqrt{\lambda_n} \right). \quad (23)$$

Proof: As in the above discussions, (22) follows from (15), (18) and $p \leq k$. The inequality in (23) holds because when one spectral component maps to another spectral component, the probability of detection will increase. \square

It can be seen from (22) and (23) that either more CRs or a smaller k will lead to better detection performance. In addition, by comparison of (6) and (23), we can see that the probability of detection increases when using either more sampling channels or higher sampling rates. Given the fact that if $M_i M_j = b > N$ (b is constant), $M_i + M_j$ can be minimized when they are consecutive primes, we choose M^1, M^2, \dots, M^v to be v consecutive prime numbers for using the fewest measurements. In such a scenario, the following approximations can be made:

$$\frac{2 \sum_{i=1}^v c^i M^i \gamma^i}{N} \simeq \frac{2 \overline{M}}{N} \sum_{i=1}^v \gamma^i = \psi \gamma_v, \quad (24)$$

$$\frac{2 \sum_{\substack{j=1 \\ i_j \in [1, v]}}^{j=k} c^{i_j} M^{i_j} \gamma^{i_j}}{N} \simeq \frac{2 \overline{M}}{N} \sum_{\substack{j=1 \\ i_j \in [1, v]}}^{j=k} \gamma^{i_j} = \psi \gamma_k \quad (25)$$

where \overline{M} is the average $c^i M^i$ over multiple CRs, $\psi \triangleq \frac{2 \overline{M}}{N}$, $\gamma_v \triangleq \sum_{i=1}^v \gamma^i$, and $\gamma_k \triangleq \sum_{\substack{j=1 \\ i_j \in [1, v]}}^{j=k} \gamma^{i_j}$.

D. Performance Over Rayleigh Fading Channels

Since CR nodes are distributed, the fading channels between the PUs and the CRs are assumed to be independent and identically distributed (i.i.d.). Considering Rayleigh fading, the SNR at CR i follows an exponential distribution. Therefore, γ_v and γ_k follow Gamma distributions given by:

$$f(\gamma_v) = \frac{(\gamma_v)^{v-1}}{(\bar{\gamma})^v \Gamma(v)} e^{-\frac{\gamma_v}{\bar{\gamma}}}, \quad \gamma_v \geq 0 \quad (26)$$

and

$$f(\gamma_k) = \frac{(\gamma_k)^{k-1}}{(\bar{\gamma})^k \Gamma(k)} e^{-\frac{\gamma_k}{\bar{\gamma}}}, \quad \gamma_k \geq 0 \quad (27)$$

where $\bar{\gamma}$ denotes local-mean SNR (SNR averaged over a few tens of wavelength), and $f(\cdot)$ denotes a genetic probability density function.

In the MSSD system, the average probabilities of false alarm and detection can be calculated by averaging $P_{f,n}$ in (22) and $P_{d,n}$ in (23) over all possible SNRs.

Theorem 2: For the proposed MSSD system operating over i.i.d. Rayleigh fading channels, the average probabilities of false alarm ($\overline{P}_{f,n}$) and detection ($\overline{P}_{d,n}$) will be bounded as

$$\frac{\Gamma(Jv, \frac{\lambda_n}{2})}{\Gamma(Jv)} \leq \overline{P}_{f,n} \leq \Theta(k, Jv, \psi, \bar{\gamma}[n], \lambda_n) \quad (28)$$

$$\overline{P}_{d,n} \geq \Theta(v, Jv, \psi, \bar{\gamma}[n], \lambda_n) \quad (29)$$

where $\Theta(x, Jv, \psi, \bar{\gamma}, \lambda)$ is defined by

$$\Theta = \left(1 + \frac{\psi \bar{\gamma}}{2}\right)^{-x} \sum_{n=0}^{\infty} C_{n+x-1}^n \left(\frac{\psi \bar{\gamma}}{\psi \bar{\gamma} + 2}\right)^n \frac{\Gamma(n+Jv, \frac{\lambda_n}{2})}{\Gamma(n+Jv)}$$

with C_a^b denoting the binomial coefficient, i.e., $C_a^b = \frac{b!}{a!(b-a)!}$.

Proof: In Rayleigh fading channels, the lower bound on the average probability of false alarm will not change as it is independent of the SNR. The upper bound of the average probability of false alarm, $\overline{P}_{f,n}^{\text{up}}$, can be evaluated by using (22), (25), and (27):

$$\overline{P}_{f,n}^{\text{up}} = \int_0^\infty Q_{Jv} \left(\sqrt{\psi \gamma_k}, \sqrt{\lambda_n} \right) \frac{(\gamma_k)^{k-1}}{(\bar{\gamma})^k \Gamma(k)} e^{-\frac{\gamma_k}{\bar{\gamma}}} d\gamma_k. \quad (30)$$

Using (4.74) in [22] and (8.352-2) in [23], we have

$$Q_{Jv} \left(\sqrt{\psi \gamma_k}, \sqrt{\lambda_n} \right) = \sum_{n=0}^{\infty} \frac{\left(\frac{\psi \gamma_k}{2}\right)^n e^{-\frac{\psi \gamma_k}{2}}}{n!} \frac{\Gamma(n+Jv, \frac{\lambda_n}{2})}{\Gamma(n+Jv)}. \quad (31)$$

Substituting (31) into (30), $\overline{P}_{f,n}^{\text{up}}$ in (30) can be written as

$$\overline{P}_{f,n}^{\text{up}} = \frac{1}{(\bar{\gamma})^k} \sum_{n=0}^{\infty} \frac{\left(\frac{\psi}{2}\right)^n \Gamma(n+Jv, \frac{\lambda_n}{2})}{n! (k-1)! \Gamma(n+Jv)} \int_0^\infty \gamma_k^{n+k-1} e^{-\frac{\psi \gamma_k}{2} - \frac{\gamma_k}{\bar{\gamma}}} d\gamma_k. \quad (32)$$

Using (3.351-3) in [23] for calculating the integral, we obtain

$$\overline{P}_{f,n}^{\text{up}} = \left(1 + \frac{\psi \bar{\gamma}}{2}\right)^{-k} \sum_{n=0}^{\infty} C_{n+k-1}^n \left(\frac{\psi \bar{\gamma}}{\psi \bar{\gamma} + 2}\right)^n \frac{\Gamma(n+Jv, \frac{\lambda_n}{2})}{\Gamma(n+Jv)}. \quad (33)$$

The lower bound on the average probability of detection can be approximated similarly. \square

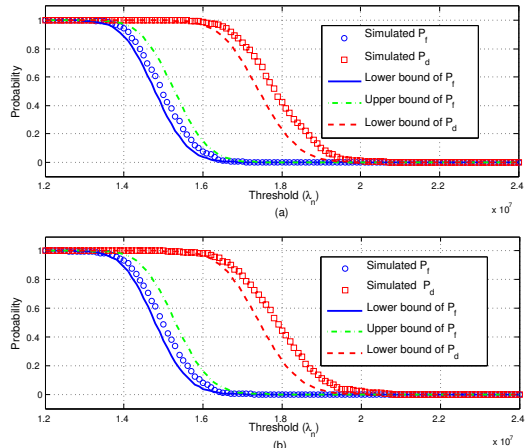


Fig. 2. Comparisons of simulation results and theoretical results for the probabilities of false alarm and detection over (a) AWGN, and (b) Rayleigh fading channels with SNR = 5 dB.

IV. SIMULATION RESULTS

In our simulations, distributed CRs are assumed to have configurations as shown in Fig. 1. The wideband signal $x^i(t)$ viewed by the CR i is assumed to be

$$x^i(t) = \sum_{l=1}^{N_b} \sqrt{E_l^i} B_l \cdot \text{sinc}(B_l(t-\Delta)) \cdot \cos(2\pi f_l(t-\Delta)) + z(t) \quad (34)$$

where $\text{sinc}(x) = \frac{\sin(\pi x)}{\pi x}$, Δ denotes a random time offset that is smaller than $T/2$, $z(t) \sim \mathcal{N}(0, 1)$, and E_l^i is the received power at CR i and varies subject to the fading channel. The wideband signal $x^i(t)$ consists of $N_b = 6$ non-overlapping subbands, whose bandwidth $B_l = 1 \sim 10$ MHz, with carrier frequency $f_l = 0 \sim 10$ GHz. Since the signal has a bandwidth of $W = 10$ GHz, if it were sampled at the Nyquist rate for $T = 0.04$ μ s, the number of Nyquist samples would be $N = 80,000$. However, in MSSD we use v sampling channels to sample the wideband signal with different sub-Nyquist rates, where $M_i \sim \mathcal{O}(\sqrt{N})$. Specifically, we select the first prime $M_1 \approx a\sqrt{N}$ ($a \geq 1$) and its $v - 1$ consecutive primes. The signal energy is calculated over an interval of $J = 50$ samples. Then 8-bit scalar quantization is performed in each CR, and these energy data are transmitted from the CRs to the FC over AWGN channels with SNR = 15 dB. In the FC, a test statistic will be formed using (14). Following [16], the compression rate is defined as M/N , where M is the average number of samples in each CR. The following figures are obtained with Matlab by using the decision rule in (15) and changing the detection threshold.

Fig. 2 compares the simulation results with the theoretical results predicted in (22)-(23) and (28)-(29). These curves are obtained by using Monte Carlo method with 100,000 trials. It is evident that the simulated probability of false alarm in all figures is close to the lower bound, but far away from the upper bound. This is due to the fact that the assumption (all k components in the full spectrum will be mirrored to the same location when the wideband signal is sub-Nyquist sampled) for deriving the upper bound has a very low probability of occurring. Fig. 3 shows the performance of MSSD over

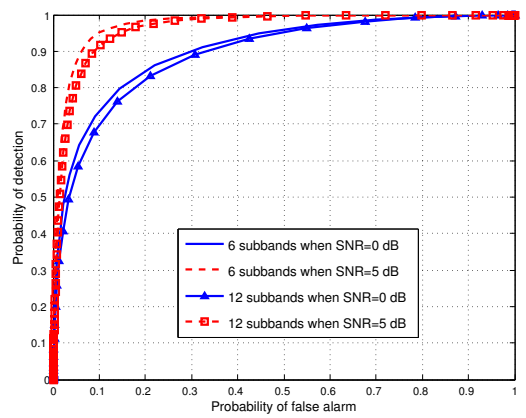


Fig. 3. Performance of MSSD over Rayleigh fading channels with $v = 22$ and $M/N = 0.0228$, when the SNR and the number of subbands vary.

i.i.d. Rayleigh fading channels with different values of k (proportional to the number of subbands). It depicts that with the same SNR, the detection performance becomes better when the number of subbands decreases. The performance improvement of MSSD stems from two phenomena. One of them is that when k decreases, the probability of signal overlap becomes smaller when the wideband signal is sub-Nyquist sampled (the signal overlap may sometimes lead to the missed detection of the PUs). The another is that, for a fixed number of sampling channels (or a fixed number of CR nodes in collaboration), decreasing k makes it easier to distinguish the occupied frequencies from the mirrored frequencies as discussed in Section III-C.

In Table I, we compare the implementation complexity of MSSD with that of the filter-bank system. The comparison metric is the number of equivalent same-speed ADCs that are required for achieving $P_d \geq 90\%$ and $P_f \leq 10\%$. For example, using 10 CRs in MSSD (each CR has one ADC with an average sampling rate of 957.54 MHz), we can obtain the above detection performance. In contrast, each CR in the filter-bank system requires 21 ADCs with the sampling rate of 957.54 MHz to cover all 10 GHz spectrum. If we consider the whole CR network, the filter-bank system employs 10×21 ADCs. In other words, the system complexity of MSSD is much less than that of the filter-bank. Another advantage of MSSD is that we can trade off (decrease) the average sampling rate of ADCs by increasing the number of sampling channels for achieving the same detection performance. This is because 40 CRs with an average sampling rate of 276.77 MHz yield similar performance to the case of 10 ADCs with an average sampling rate of 957.54 MHz. Fig. 4 shows the performance comparison of MSSD and the CS-based system [16] over Rayleigh fading channels. We can see that MSSD outperforms the CS-based system for both compression rates. Additionally, it can be seen that both systems have better detection performance when the compression rate increases. Furthermore, we find that the computational complexity of MSSD (similar to energy detection) is $\mathcal{O}(N)$, instead of $\mathcal{O}(MN)$ in the CS-based system (due to matrix multiplications for spectrum recovery [16]). Hence, with either limited computational resources at the FC or restricted bandwidth for

TABLE I
COMPLEXITY COMPARISON OF MSSD AND THE FILTER-BANK SYSTEM
OVER RAYLEIGH FADING CHANNELS WITH ZERO DECIBEL SNR.

Number of CRs in collaboration (v)	10	20	30	40
Number of ADCs using MSSD	10×1	20×1	30×1	40×1
Number of ADCs using filter-bank	10×21	20×40	30×58	40×74
Average sampling rate of ADC (MHz)	957.54	513.08	350.34	276.77

sharing spectrum sensing data, MSSD will result in a lower spectrum sensing overhead than the CS-based system.

V. CONCLUSIONS

In this paper, we have proposed a novel system, MSSD, for cooperative wideband spectrum sensing in distributed CR networks. It has been shown that MSSD can significantly decrease the spectrum sensing requirements of CRs thanks to the parallel sub-Nyquist samplings with different sampling rates. We have shown that using a few sub-Nyquist samples, the wideband spectrum can be sensed without full spectrum recovery, which results in a high energy-efficiency and a low spectrum sensing overhead. In addition, we have analyzed and derived some closed-form bounds for the performance of MSSD over both non-fading and Rayleigh fading channels.

Simulation results have shown that the derived bounds for the probabilities of false alarm and detection can closely fit the simulated curves. It has also been shown that using only a few measurements, MSSD performs well under low SNR scenarios over Rayleigh fading channels. The performance of MSSD becomes better when either the number of CRs or the average sampling rate increases. Compared with existing technologies, we have found that MSSD not only has a lower complexity, but also has a better detection performance in the fading scenario, even if the compression rate is extremely low. Such an MSSD system is not limited to wideband spectrum sensing system in CR, as the same principles could easily be used to design a broadband spectral analyzer, and a signals-intelligence receiver. The performance analysis of MSSD over other fading channels, e.g., Nakagami fading, slow fading, and Rician fading, is left as future work.

REFERENCES

- [1] FCC, "Spectrum Policy Task Force," 11/2002, ET Docket 02-135.
- [2] J. Mitola, "Cognitive radio: An integrated agent architecture for software defined radio," Ph.D. dissertation, Dept. of Teleinformatics, Royal Institute of Technology, Stockholm, Sweden, 8 May, 2000.
- [3] H. Sun, D. Laurenson, J. Thompson, and C.-X. Wang, "A novel centralized network for sensing spectrum in cognitive radio," in *Proc. IEEE International Conference on Communications*, Beijing, China, May 2008, pp. 4186–4190.
- [4] C.-X. Wang, H.-H. Chen, X. Hong, and M. Guizani, "Cognitive radio network management: tuning in to real-time conditions," in *IEEE Veh. Tech. Mag.*, vol. 3, no. 1, Mar. 2008, pp. 28–35.
- [5] C.-X. Wang, X. Hong, H.-H. Chen, and J. Thompson, "On capacity of cognitive radio networks with average interference power constraints," *IEEE Trans. Wireless Comm.*, vol. 8, no. 4, pp. 1620–1625, Apr. 2009.
- [6] X. Hong, C.-X. Wang, H.-H. Chen, and Y. Zhang, "Secondary spectrum access networks: recent developments on the spatial models," *IEEE Veh. Techno. Magazine*, vol. 4, no. 2, pp. 36–43, June 2009.
- [7] T. Cui, F. Gao, and A. Nallanathan, "Optimization of cooperative spectrum sensing in cognitive radio," *IEEE Trans. on Vehicular Technology*, vol. 60, no. 4, pp. 1578–1589, May 2011.
- [8] Q. Chen, F. Gao, A. Nallanathan, and Y. Xin, "Improved cooperative spectrum sensing in cognitive radio," in *Proc. IEEE Vehicular Technology Conference*, Singapore, May 2008, pp. 1418–1422.
- [9] Q. Chen, M. Motani, W.-C. Wong, and A. Nallanathan, "Cooperative spectrum sensing strategies for cognitive radio mesh networks," *IEEE Journal of Selected Topics in Signal Processing*, vol. 5, no. 1, pp. 56–67, Feb. 2011.
- [10] Z. Tian and G. B. Giannakis, "A wavelet approach to wideband spectrum sensing for cognitive radios," in *Proc. 1st CrownCom*, Mykonos Island, Greece, 2006, pp. 1–5.
- [11] Z. Quan, S. Cui, A. Sayed, and H. Poor, "Optimal multiband joint detection for spectrum sensing in cognitive radio networks," *IEEE Trans. Signal Processing*, vol. 57, no. 3, pp. 1128–1140, Mar. 2009.
- [12] Z. Quan, S. Cui, A. H. Sayed, and H. Poor, "Wideband spectrum sensing in cognitive radio networks," in *Proc. IEEE International Conference on Communications*, Beijing, China, 2008, pp. 901–906.
- [13] B. Farhang-Boroujeny, "Filter bank spectrum sensing for cognitive radios," *IEEE Trans. Signal Processing*, vol. 56, no. 5, pp. 1801–1811, 2008.
- [14] Z. Tian and G. B. Giannakis, "Compressed sensing for wideband cognitive radios," in *Proc. IEEE International Conference on Acoustics, Speech, and Signal Processing*, Honolulu, 2007, pp. 1357–1360.
- [15] Y. L. Polo, Y. Wang, A. Pandharipande, and G. Leus, "Compressive wide-band spectrum sensing," in *Proc. IEEE International Conference on Acoustics, Speech, and Signal Processing*, Taipei, 2009, pp. 2337–2340.
- [16] Y. Wang, A. Pandharipande, Y. L. Polo, and G. Leus, "Distributed compressive wide-band spectrum sensing," in *Proc. Information Theory and Applications Workshop*, San Diego, Feb. 2009, pp. 178–183.
- [17] H. Sun, D. Laurenson, and C.-X. Wang, "Computationally tractable model of energy detection performance over slow fading channels," *IEEE Comm. Letters*, vol. 14, no. 10, pp. 924–926, Oct. 2010.
- [18] F. F. Digham, M.-S. Alouini, and M. K. Simon, "On the energy detection of unknown signals over fading channels," in *Proc. IEEE International Conference on Communications*, Anchorage, 2003, pp. 3575–3579.
- [19] M. A. McHenry, "NSF spectrum occupancy measurements project summary," Shared Spectrum Company, Tech. Rep., Aug. 2005.
- [20] Y. Youn, H. Jeon, J. H. Choi, and H. Lee, "Fast spectrum sensing algorithm for 802.22 WRAN systems," in *Proc. International Symposium on Communications and Information Technologies*, Bangkok, Thailand, Sep. 2006, pp. 960–964.
- [21] W. A. Gardner, *Statistical Spectral Analysis a Nonprobabilistic Theory*. New York: Prentice-Hall, Inc., 1986.
- [22] M. K. Simon and M.-S. Alouini, *Digital Communication over Fading Channels*, 2nd ed. New York: John Wiley & Sons, Inc., Dec. 2004.
- [23] I. S. Gradshteyn and I. M. Ryzhik, *Table of Integrals, Series, and Products*, 5th ed., A. Jeffrey, Ed. New York: Academic Press, Inc., 1994.

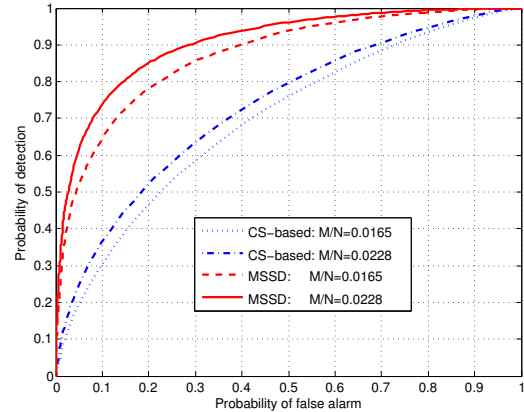


Fig. 4. Comparison of MSSD and CS-based system over Rayleigh fading channels with $\text{SNR} = 0 \text{ dB}$ and $v = 22$, when the compression rate M/N varies.